

Anisotropic strain relaxation of Ge nanowires on Si(113) studied by medium-energy ion scatteringKoji Sumitomo,* Hiroo Omi, Zhaohui Zhang,[†] and Toshio Ogino*NTT Basic Research Laboratories, NTT Corporation, Atsugi, Kanagawa 243-0198, Japan*

(Received 9 September 2002; revised manuscript received 21 October 2002; published 22 January 2003)

We have investigated the strain state in Ge nanowires on Si(113) substrate using medium-energy ion scattering. We found that nanowires have negligibly relaxed compressive strain along their length, but the strain across them is almost totally relaxed. Anisotropic strain relaxation plays a role in determining the width of the nanowires.

DOI: 10.1103/PhysRevB.67.035319

PACS number(s): 68.55.Jk, 81.15.Hi, 68.49.Sf

I. INTRODUCTION

The Ge/Si heteroepitaxial system has been studied extensively for device application. As is well known, Ge grows on the Si surface in the Stranski-Krastanow (SK) mode to relax the strain caused by the lattice mismatch between Ge and Si. Elastic strain is one of the most significant factors governing the surface morphologies, structures, and properties.¹ For control of self-assembling Ge islands on the Si substrate, sufficient understanding of strain relaxation is indispensable. For the self-assembly of quantum dots on a Si(001) surface, the formation of well-ordered Ge nanocrystals and subsequent shape transition have been studied extensively for the last decade.^{2,3} Two typical Ge nanocrystal shapes, depending on their size, are square-based pyramids bounded by {105} facets for smaller volume and domes with a complex geometry of steeper facets. The shape transition from pyramids to domes results from the interplay between strain relaxation at the facets and stress concentration at the edges.^{2,4} For the formation of Ge or Ge-Si quantum wires, however, C_{1v} symmetry Si(113) seems to be more attractive because of its anisotropy. Ge grown epitaxially on Si(113) can form highly elongated three-dimensional (3D) islands along the $[33\bar{2}]$ direction, which are candidates for the self-assembled quantum wires.⁵⁻⁷ The relation between the surface and bulk anisotropy and the nanowire formation has been reported.⁸⁻¹⁰ Once nucleation of three-dimensional islands begins, it has been suggested that the interplay between anisotropic strain relaxation and kinetic influences becomes dominant.¹¹ However, no strain measurements have ever been made in detail necessary to understand the role of anisotropic strain relaxation in the nanowire formation.

This paper describes the strain distribution of Ge nanowires grown on Si(113) substrate, which we investigated using medium-energy ion scattering (MEIS). MEIS is one of the most powerful techniques for determining the atomic displacement quantitatively.¹²⁻¹⁴ From MEIS blocking profiles measured along and across the Ge nanowires, we could analyze the strain relaxation quantitatively. We discuss the relation between the anisotropic strain relaxation and the nanowire stabilization mechanism.

II. EXPERIMENT

Sample preparation and MEIS measurements were carried out in an ultrahigh-vacuum (UHV) system consisting of

three working chambers for MEIS, molecular-beam epitaxy (MBE), and photoelectron spectroscopy. The system is described in detail elsewhere.¹⁵ The samples prepared in the MBE chamber can be transferred to the MEIS chamber in the UHV. Si(113) wafers with a dimension of $15 \times 17 \text{ mm}^2$ (P doped, $\rho = 1-10 \text{ } \Omega \text{ cm}$) were preoxidized chemically and introduced into the UHV through a load lock. After outgassing at 620°C for 1–2 h, the samples were heated from behind to 850°C by radiation from a W filament to remove the protective oxides. The sample temperature was measured using an infrared pyrometer. The samples were then cooled to the Si buffer-growth temperature of 620°C . Si buffer layers were deposited at 0.5–1.0 nm/min using a 10-kV electron-beam evaporator. After deposition of a Si buffer layer 10–15 nm thick and annealing at 850°C , clean and flat Si(113) surfaces were confirmed by reflection high-energy electron diffraction. Ge was deposited at a rate of 0.6–0.7 ML/min, where 1 ML is defined as $8.2 \times 10^{14} \text{ atoms/cm}^2$, using a Knudsen cell operated at 1180°C . The growth temperature was 430°C to favor nanowire formation.^{6,7} The base pressure of the MBE chambers is $3 \times 10^{-11} \text{ Torr}$, and the respective pressures when evaporating Si and Ge were below 3×10^{-9} and $5 \times 10^{-10} \text{ Torr}$. Carbon contamination during Si and Ge growth was confirmed to be less than detection limit of Auger electron spectroscopy and x-ray photoelectron spectroscopy.

In the MEIS measurements, a H^+ ion beam of 99.5 keV energy was used for the probe. The energy and scattering angle of backscattered ions were analyzed with a two-dimensional detector,¹⁶ whose energy resolution $\Delta E/E$ is about 3×10^{-3} and angle resolution is 0.1° . For analysis of the strain in the 3D islands, the planar channeling geometries were adopted in order to detect the ions scattered from the core of the islands. After MEIS measurements, antiferromagnetic *ex situ* observations were carried out using a Digital Instruments Nanoscope III to confirm the surface morphology. The nanowires are along $[33\bar{2}]$ and their typical geometries are 20 nm in width, 1–5 nm in height, and several hundred nanometers or more than $1 \text{ } \mu\text{m}$ in length.

III. RESULTS AND DISCUSSION

When Ge is deposited on the Si(113) substrate, as described in previous reports,^{5-7,10} nucleation of 3D islands begins after 5-ML 2D wetting layer growth. Figure 1 shows the MEIS energy spectra obtained from the Ge thin films

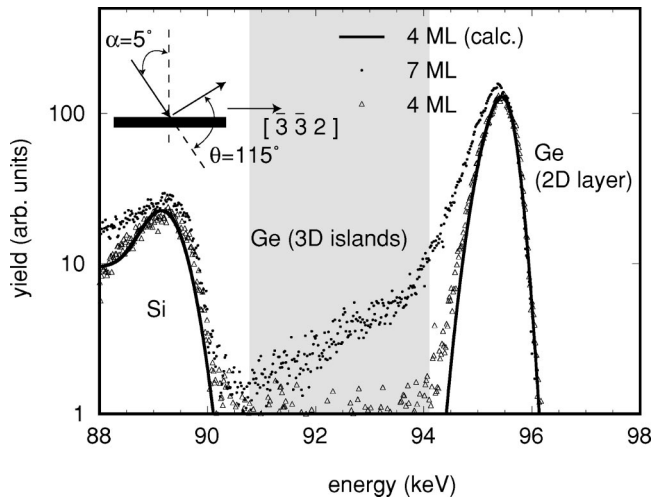


FIG. 1. MEIS energy spectra from the 7- and 4-ML Ge deposited on the Si(113) surface.

grown on Si(113) substrate. The amounts of Ge deposited were 4 and 7 ML before and after the nucleation of 3D islands started, respectively. The incident angle of the probe ion was set to 5° from the surface normal in order to get information on deeper layers. In this scattering geometry, we can analyze the strain inside Ge 3D islands. The scattering angle was 115° and the scattering plane was $(1\bar{1}0)$. It is confirmed that Ge thin films grew in the typical Stranski-Krastanow growth mode on Si(113) surface. From the 4-ML Ge surface, we can see the clear Ge peak that corresponds to the Ge two-dimensional layer. The solid line represents the simulated spectrum for the 4-ML Ge thin film that is two-dimensionally grown on the Si substrate. The simulated spectrum is consistent with the experimental one. When Ge is deposited to more than the critical thickness,⁶ the Ge 3D islands form on the 2D layer. The peak intensity of the MEIS energy spectra for Ge 2D layer is not changed so much and an obvious tailing on low-energy side appears. The ions scattered from the inside of the 3D islands are distributed between 91 and 94 keV.

For a heteroepitaxial system such as Ge/Si, intermixing and interdiffusion between Ge thin film and Si substrate often play important roles in surface morphological change. Henstrom *et al.* showed the strain enhanced interdiffusion at the 3D islands on Ge/Si(001) system.¹⁷ In our case, however, such effects are not remarkable because our growth temperature (430°C) is much lower than theirs (650°C). The intermixing and interdiffusion are estimated from MEIS energy spectra. Figure 2 shows the surface peaks of Si in the MEIS energy spectrum measured for Ge(4 ML)/Si(113) in the channeling geometry. The incident angle α was set at 64.76° , which corresponds to the $[110]$ channeling direction, and the scattering angle θ was 90° . The experimental spectrum is compared with the theoretical calculations for two plausible models: one having complete abrupt interface (model 1) and the other having 20% of the Si atoms segregated at the topmost surface (model 2). The experimental spectrum shows the clear surface peak that is formed by ions scattered from several atomic layers at the interface and is in

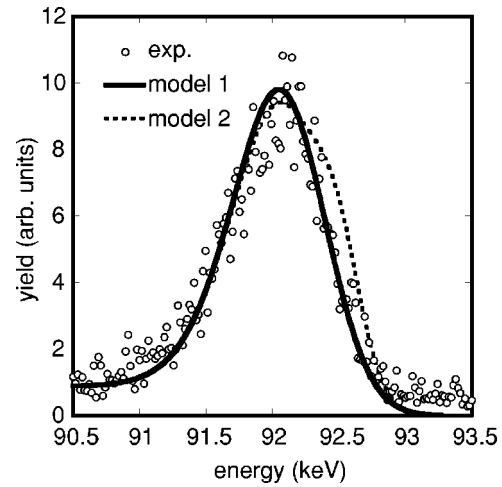


FIG. 2. The surface peaks of Si in the MEIS energy spectrum measured for Ge(4 ML)/Si(113) in the channeling geometry along the $[110]$ direction. The experimental spectrum is compared with theoretical calculations for two plausible models: one having a complete abrupt interface (model 1) and the other having 20% of the Si atoms segregated at the topmost surface (model 2).

agreement with the calculation for model 1. The present results suggest that, within the permitted depth resolution of MEIS (0.1 nm order), the interface between Ge and Si is abrupt. We do not have to consider any intermixing in the 3D islands.

In order to analyze the strain distribution, we measured MEIS blocking profiles in two typical scattering planes; one along the $[3\bar{3}\bar{2}]$ direction, i.e., parallel to Ge nanowires, and the other along $[1\bar{1}0]$, i.e., across Ge nanowires. Figure 3 shows the blocking profile for Ge signals of nanowires measured parallel to the nanowires. The $(1\bar{1}0)$ planar channeling geometry was adopted. The incident angle of the probe ion was 5° from normal, as shown in the inset of Fig. 3. The

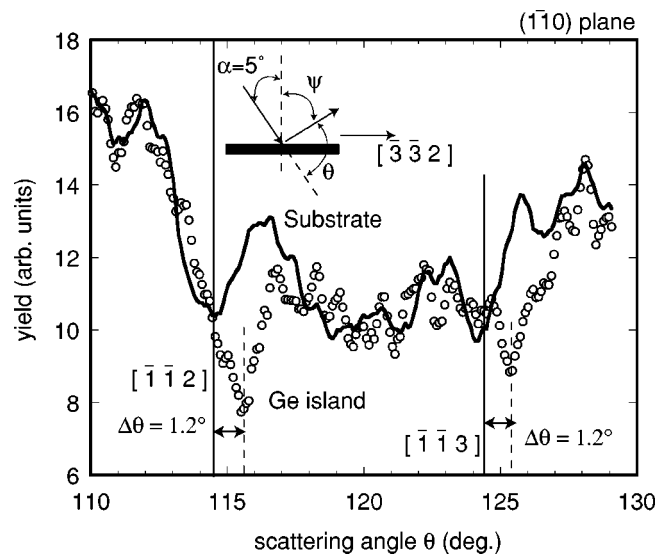


FIG. 3. Blocking profile for Ge nanowires measured in the $(1\bar{1}0)$ plane; that for the Si substrate is shown for reference.

scattered ions were collected around $[\bar{1}\bar{1}2]$ between 110° and 130° . In order to remove the contribution of the surface reconstruction at the wetting layer, the integration range to obtain blocking profiles was selected as yields corresponding to the signal scattered from Ge atoms between 1 and 5 nm deep, which appears at energies lower than the surface peak. The Si substrate (between 3 and 10 nm deep) is shown for reference. In the blocking profile of the Si substrate, we can see clear blocking dips at 114.5° and 124.5° . These dips are in agreement with the calculated angle for $[\bar{1}\bar{1}2]$ and $[\bar{1}\bar{1}3]$ directions, respectively.

Similar blocking dips in the blocking profiles of the Ge nanowires were also observed. However, the angles of the dips were a little bit higher than those for the Si substrate. These angle shifts indicate that the Ge atoms of the inner Ge nanowires are displaced from the ideal lattice site. Ge layer and islands are strained compressively laterally and expand vertically because the lattice constant of Ge is about 4% larger than that of Si. From the difference of these dip angles between the Si bulk and Ge nanowires ($\Delta\theta=1.2^\circ$), the vertical strain (ε_z) can be estimated as

$$\frac{(1+\varepsilon_z)}{(1+\varepsilon_x)} = \frac{\cot(\psi+\Delta\psi)}{\cot\psi}, \quad (1)$$

where ψ is an ideal exit angle measured from surface normal, which is expected from the nonstrained crystal, and $\Delta\psi = -\Delta\theta$ is the angle shift. The Ge layer and islands are strained compressively laterally. The length of nanowires along $[3\bar{3}\bar{2}]$ is more than 500 nm and signs of dislocations are not observed in scanning tunneling microscopy (STM) and cross-sectional TEM images.¹⁸ Therefore, the lattice constant along $[3\bar{3}\bar{2}]$ can be regarded to be same as that for the Si substrate, i.e., $(1+\varepsilon_x) = a_{Si}/a_{Ge}$. The vertical expansion is caused by the compressive strain along the nanowires, ε_z is calculated to be 0.7 and 0.2%, for $[\bar{1}\bar{1}2]$ and $[\bar{1}\bar{1}3]$ dips, respectively. The uncertainty caused by the angle resolution $\pm 0.1^\circ$ of our 2D detector is about $\pm 0.5\%$, and must be the main reason for the disagreement in the calculation between the two blocking dips.

Compressive strain along $[1\bar{1}0]$, which is the direction across the nanowires, is also expected. In order to estimate the strain, we also observed the blocking profiles in the $(3\bar{3}\bar{2})$ scattering plane as shown in Fig. 4. The incident angle of the probe ion was 25° from normal. The scattering angle was set between 110° and 125° . The most remarkable result is that the blocking dips from Ge nanowires are consistent with their angles from the substrate. We can see clear blocking dips at 114.5° and 122.5° in the blocking profiles for both the Si substrate and Ge nanowires. These blocking angles correspond to the $[3\bar{1}3]$ and $[5\bar{1}6]$ directions. Almost the same strain ε_y along $[1\bar{1}0]$ as the vertical strain ε_z is calculated from Eq. (1). This indicates that the compressive strain along $[1\bar{1}0]$ is almost totally relaxed and tensile strain is produced instead. Schematic illustrations of the strain distribution along and across the nanowires are shown in Fig. 5. Since the width of nanowires is much smaller than

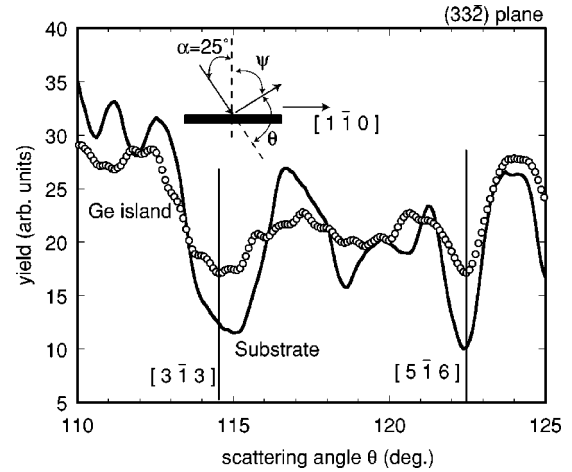


FIG. 4. Blocking profile for Ge nanowires measured in the $(3\bar{3}\bar{2})$ plane; that for the Si substrate is shown for reference.

their length, it is easy to relieve the strain across the nanowire. Abrupt strain relaxation at the interface is unreasonable because the misfit between the relaxed Ge and the Si substrate is too large. The estimated misfit (1 nm) is larger than the interlayer distance (0.384 nm) along $[1\bar{1}0]$. The strain must be relaxed gradually layer by layer. Finally, the compressive strain across the nanowires is almost totally relaxed. The estimated tensile strain of $\varepsilon_z = \varepsilon_y = (0.5 \pm 0.5)\%$ is consistent with that obtained from the simple calculation with Poisson's ratio $\nu = 0.3$ under uniaxial stress along nanowires caused by lattice mismatch between Si and Ge.

The average width, height, and length of the nanowires as a function of Ge deposited are shown in Fig. 6. Their width is almost constant at 20 nm, even if the amount of deposited Ge increases in the initial stage of nanowire formation. Furthermore, STM images¹⁰ have shown highly uniform distribution of nanowire width. The nanowire growth is characterized by an increase of length with Ge deposition. The relaxation across the nanowires determines the upper limit of the nanowire width. Therefore, the nanowire width saturates in the initial stage of the 3D-island formation. The height of the nanowires is also restricted by the free energy of the

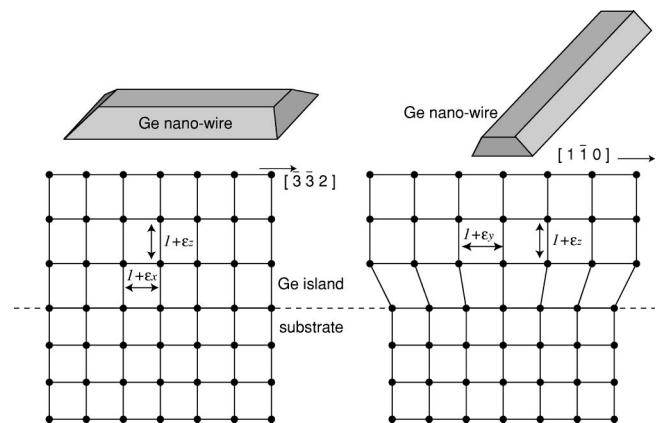


FIG. 5. Schematic illustration of strain along and across the nanowires.

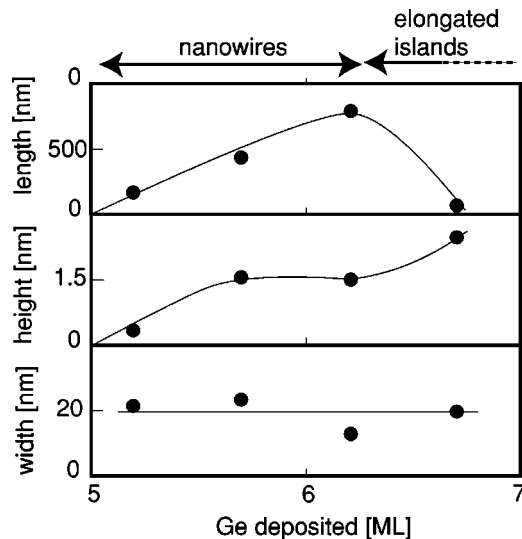


FIG. 6. The average width, height, and length of the nanowires as a function of Ge deposited, measured from STM wide-scan images ($0.9 \times 0.9 \mu\text{m}^2$). Solid curves are eye guides.

(159) side facets, when the width is fixed. These restrictions of the width and height make possible the full strain relaxation across the nanowires. Strain relaxation across the nanowires leads to additional compressive strain in the wet-

ting layer. As described in previous reports,^{10,11} the depression of the wetting layer in the STM image was observed next to the side edges of nanowires. In order to relieve the additional compressive strain, trenches are formed, which inhibit the increase of nanowire width. Anisotropic strain relaxation in Ge nanowires stabilizes the elongated growth of the 3D islands.

IV. SUMMARY

We have investigated the strain state in Ge nanowires grown on a Si(113) substrate. MEIS blocking profiles measured along and across the Ge nanowires show that the nanowires have compressive strain along them and the strain across them is almost totally relaxed. The vertical expansion caused by the compressive strain along the nanowires is estimated to be $(0.5 \pm 0.5)\%$, which is consistent with that obtained from an anisotropic elasticity calculation of uniaxial stress along a nanowire caused by lattice mismatch between Si and Ge. The results clearly demonstrate a relation between the anisotropic strain relaxation and the stabilization of the elongated growth of 3D islands on heteroepitaxial systems.

ACKNOWLEDGMENTS

We thank David J. Bottomley and Kuniyil Prabhakaran for many stimulating discussions.

*Email address: sumitomo@will.brl.ntt.co.jp; <http://www.brl.ntt.co.jp/people/sumitomo>

[†]Permanent address: Mesoscopic Physics National Laboratory and Department of Physics, Peking University, Beijing 100871, China.

¹J. Tersoff and R.M. Tromp, Phys. Rev. Lett. **70**, 2782 (1993).

²G. Medeiros-Ribeiro, A.M. Bratkovski, T.I. Kamins, D.A.A. Ohlberg, and R.S. Williams, Science **279**, 353 (1998).

³F.M. Ross, J. Tersoff, and R.M. Tromp, Phys. Rev. Lett. **80**, 984 (1998).

⁴C.P. Liu, J.M. Gibson, D.G. Cahill, T.I. Kamins, D.P. Basile, and R.S. Williams, Phys. Rev. Lett. **84**, 1958 (2000).

⁵J. Knall and J.B. Pethica, Surf. Sci. **265**, 156 (1992).

⁶H. Omi and T. Ogino, Phys. Rev. B **59**, 7521 (1999).

⁷H. Omi and T. Ogino, Appl. Phys. Lett. **71**, 2163 (1997).

⁸D.J. Bottomley, H. Omi, and T. Ogino, J. Cryst. Growth **225**, 16 (2001).

⁹Z. Zhang, K. Sumitomo, J. Nakamura, H. Omi, A. Natori, and T.

Ogino, Phys. Rev. Lett. **88**, 256101 (2002).

¹⁰Z. Zhang, K. Sumitomo, H. Omi, and T. Ogino, Surf. Sci. **497**, 93 (2002).

¹¹K. Sumitomo, Z. Zhang, H. Omi, D.J. Bottomley, and T. Ogino, J. Cryst. Growth **237-239**, 1904 (2002).

¹²J.F. van der Veen, Surf. Sci. Rep. **5**, 199 (1985).

¹³K. Sumitomo, T. Nishioka, and T. Ogino, J. Vac. Sci. Technol. B **13**, 387 (1995).

¹⁴S.J. Kahng, Y.H. Ha, D.W. Moon, and Y. Kuk, Phys. Rev. B **61**, 10 827 (2000).

¹⁵K. Sumitomo, T. Nishioka, N. Shimizu, Y. Shinoda, and T. Ogino, J. Vac. Sci. Technol. A **13**, 289 (1995).

¹⁶R.M. Tromp, M. Copel, M.C. Reuter, M.H. von Hoegen, J. Speidell, and R. Koudis, Rev. Sci. Instrum. **62**, 2679 (1991).

¹⁷W.L. Henstrom, C.P. Liu, J.M. Gibson, T.I. Kamins, and R.S. Williams, Appl. Phys. Lett. **77**, 1623 (2000).

¹⁸Z. Zhang, K. Sumitomo, H. Omi, and T. Ogino (unpublished).